PROBLEMY KOLEJNICTWA
RAILWAY REPORT Issue 185 (December 2019)
DOI: 10.36137/1856E
ISSN 0552-2145 (print) ISSN 2544-9451 (on-line)

Transition Curves on Railway Roads in Terms of Feasibility

Władysław KOC[1]

Summary
The work first addressed the issue of accepting limit values for kinematic parameters on railway roads, demonstrating that it is appropriate to maintain the same rules for all types of transition curves. Then, the prevailing opinion about the reason for the limited scope of application of the so-called smooth transition curves was confirmed. These curves have one major disadvantage – very small values of horizontal ordinates (and ordinates of the gradient due to cant) in the initial region, in practice often impossible to implement and then maintain. The main part of the work was devoted to the determination of a new form of transition curve, which – in contrast to the commonly used clothoid – is characterized by a gentle curvature in the area of entry into the circular arc. A clear advantage of this curve (from the implementation point of view) over the smooth transition curves of the Bloss curve was demonstrated.

Keywords: railway, timetable, schedule, conductor teams

1. Introduction

The issue of transition curves on roads for motor vehicles and railways is still topical. New curve forms are constantly being sought [1, 35, 78, 19, 25, 27–29, 33]. Among Polish researchers, A. Kobryń [10–14] broadly deals with this issue on roads for motor vehicles, while K. Zboiński's team with railway roads, which also took into account the dynamic model of the system: rail vehicle – track [31, 32].The conducted research is undoubtedly very interesting and, to a large extent, develops the theory of the discussed issue. They point to the benefits that would be provided by practical application of the proposed solutions. The Wiener Bögen transition curve developed in Austria [9, 30] has even been patented.

Unfortunately, the common feature of the search for new forms of transition curves carried out over the last few decades is the lack of a solution that would be accepted in practice and widely implemented. The clothoid, with its linear curvature, still plays a dominant role in the geometrical systems of communication routes. Its basic disadvantage is the deflections on the curvature diagram, occurring in the initial and final regions, which are the cause of adverse dynamic interactions in the track – rail vehicle system. On railway roads, the third-degree parabola, being a simplification of the clothoid, is still used, and this simplification, with the current calculation possibilities, has no justification at all.

The acceleration values along the length of the transition curve result from the distribution of curvature, which should be the basis for the identification of transition curves. In general, it can be linear or non-linear. For non-linear curvature change, the term "smooth transition curves", used by R.J. Grabowski [6], corresponding to the key importance of the function class describing curvature, seems appropriate. Most transition curves combine a common algorithm for curvature determination using differential equations [16–18, 24].

It should be noted that there is a certain group of smooth transition curves that have been recognised on the railways and are present in the current design rules. They have a long history dating back to the first half of the 20th century, but their scope of application is still limited. In Poland, they were propagated in a fundamental book by H. Bałuch [2]. The characteristics of the following curves are presented there: fourth-degree parabola, the Bloss curve, the cosine and sinusoidal curves. Comparative analysis of the transition curves mentioned above was the subject of some works [15, 22].

[1] Prof. Ph.D. D.Sc. Eng.: Gdańsk University of Technology, Rail Transport and Bridges; e-mail: kocwl@pg.edu.pl.

2. Acceptance of limit values for kinematic parameters

On railway roads, the mutual comparison of transition curves requires certain assumptions to be made regarding the applicable values of the permissible kinematic parameters – the acceleration increment ψ and the speed of rolling stock wheel lifting on the gradient due to cant f. There is an intuitive conviction that much higher (even doubled) limit values can be assumed for smooth transition curves than for the clothoid (since the maximum values ψ and f occur only in the central part of these curves and they are much smaller in the extreme parts). This was reflected in the binding regulations in Poland [26], however, it is questionable.

The kinematic parameters ψ and f on transition curves and gradients due to cant can be described using the following general formulae:

$$\psi(l) = \frac{a_m V}{3{,}6}\frac{d}{dl}g(l), \tag{1}$$

$$f(l) = \frac{h_0 V}{3{,}6}\frac{d}{dl}g(l), \tag{2}$$

where:

V – train speed in km/h,
a_m – unbalanced acceleration on a circular curve in m/s^2,
h_0 – cant value on a circular curve in mm,
l – variable defining the position of a given point on the transition curve in m,
$g(l)$ – function of variable l related to the curvature of a given transition curve (value without unit).

The $g(l)$ function depends on the type of transition curve. For the mentioned curves from [2], if we determine their length by l_k, equations $g(l)$ and $\frac{d}{dl}g(l)$ are as follows:

for the clothoid:

- for a fourth-degree parabola:

$$g(l) = \frac{l}{l_k},\ \frac{d}{dl}g(l) = \frac{1}{l_k};$$

- for the Bloss curve:

$$g(l) = 2\left(\frac{l}{l_k}\right)^2,\ \frac{d}{dl}g(l) = \frac{4}{l_k}\frac{l}{l_k},\ l \in \left\langle 0, \frac{l_k}{2}\right\rangle,$$

$$g(l) = -1 + 4\frac{l}{l_k} - 2\left(\frac{l}{l_k}\right)^2,\ \frac{d}{dl}g(l) = \frac{4}{l_k}\left(1 - \frac{l}{l_k}\right),$$

$$l \in \left\langle \frac{l_k}{2}, l_k\right\rangle;$$

- for the cosine curve:

$$g(l) = 3\left(\frac{l}{l_k}\right)^2 - 2\left(\frac{l}{l_k}\right)^3,\ \frac{d}{dl}g(l) = \frac{6}{l_k}\left[\frac{l}{l_k} - \left(\frac{l}{l_k}\right)^2\right];$$

- for the sine curve:

$$g(l) = \frac{l}{l_k} - \frac{1}{2\pi}\sin\left(2\pi\frac{l}{l_k}\right),$$

$$\frac{d}{dl}g(l) = \frac{1}{l_k}\left[1 - \cos\left(2\pi\frac{l}{l_k}\right)\right].$$

The equations (1) and (2) imply that:

$$3{,}6\frac{\psi(l)}{a_m V} = 3{,}6\frac{f(l)}{h_0 V} = \frac{d}{dl}g(l), \tag{3}$$

which, for the transitional curves concerned, leads to the following relationships:

- for the clothoid:

$$\psi(l)\cdot\frac{3{,}6 l_k}{a_m V} = f(l)\cdot\frac{3{,}6 l_k}{h_0 V} = 1;$$

- for a fourth-degree parabola:

$$\psi(l)\cdot\frac{3{,}6 l_k}{a_m V} = f(l)\cdot\frac{3{,}6 l_k}{h_0 V} = 4\frac{l}{l_k},\ l \in \left\langle 0, \frac{l_k}{2}\right\rangle,$$

$$\psi(l)\cdot\frac{3{,}6 l_k}{a_m V} = f(l)\cdot\frac{3{,}6 l_k}{h_0 V} = 4\left(1 - \frac{l}{l_k}\right),\ l \in \left\langle \frac{l_k}{2}, l_k\right\rangle;$$

- for the Bloss curve:

$$\psi(l)\cdot\frac{3{,}6 l_k}{a_m V} = f(l)\cdot\frac{3{,}6 l_k}{h_0 V} = 6\left[\frac{l}{l_k} - \left(\frac{l}{l_k}\right)^2\right];$$

- for the cosine curve:

$$\psi(l)\cdot\frac{3{,}6 l_k}{a_m V} = f(l)\cdot\frac{3{,}6 l_k}{h_0 V} = \frac{\pi}{2}\sin\left(\pi\frac{l}{l_k}\right);$$

- for the sine curve:

$$\psi(l)\cdot\frac{3,6l_k}{a_m V}=f(l)\cdot\frac{3,6l_k}{h_0 V}=1-\cos\left(2\pi\frac{l}{l_k}\right).$$

The relationships are presented graphically in Figure 1. It is evident that exceeding the values ψ and f occurring on the clothoid is not local (point), but covers at least half of the length of the considered smooth transition curves, and the value of this excess is significant. The intervals of the variable l/l_k while exceeding the values ψ and f are as follows:

- for a fourth-degree parabola and the sine curve
  - $l/l_k \in (0,25;0,75)$,
- for the Bloss curve
  - $l/l_k \in \left(0,5-\sqrt{3}/6;0,5+\sqrt{3}/6\right)$, e.i. $l/l_k \in (0,211;0,789)$
- for the cosine curve
  - $l/l_k \in \left(\arcsin(2/\pi)/\pi;1-\arcsin(2/\pi)/\pi\right)$, e.i. $l/l_k \in (0,22;0,78)$.

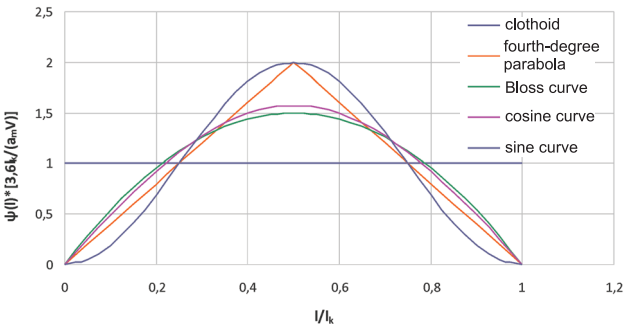

Fig. 1. The values $\psi(l)\cdot\frac{3,6l_k}{a_m V}\left(f(l)\cdot\frac{3,6l_k}{h_0 V}\right)$ on the length of the considered transition curves [own study]

For this reason too, it seems appropriate to maintain the same rules on the limit values for kinematic parameters for all types of transitional curves. The assumption of the same values for ψ_{per} *and* f_{per} leads to the need to extend the individual smooth transition curves in relation to the clothoid (by introducing an appropriate A coefficient resulting from an overrun value of ψ and f at the centre of the curve). It is then possible to compare the horizontal ordinates of transition curves and gradients due to cant transition ordinates. The A-coefficient values are as follows:

- for a fourth-degree parabola $A = 2$,
- for the Bloss curve $A = 3/2$,
- for the cosine curve $A = \pi/2$,
- for the sine curve $A = 2$.

3. Horizontal ordinates of transition curve and gradient due to cant ordinates in the initial region

One paper [18] presented an analysis of the considered forms of smooth transition curves. The identification of $k(l)$ curvature for particular curves by means of differential equations was made, the parametric equations $x(l)$ and $y(l)$ were determined and the list of these equations was presented:

- for the clothoid:

$$k(l)=\frac{1}{Rl_k}l, \tag{4}$$

$$x(l)=l-\frac{1}{40R^2l_k^2}l^5+\frac{1}{3456R^4l_k^4}l^9-\frac{1}{599040R^6l_k^6}l^{13}, \tag{5}$$

$$y(l)=\frac{1}{6Rl_k}l^3-\frac{1}{336R^3l_k^3}l^7+\frac{1}{42240R^5l_k^5}l^{11}; \tag{6}$$

- for a fourth-degree parabola:
  - within $l\in\left\langle 0,\frac{l_k}{2}\right\rangle$:

$$k(l)=\frac{2}{Rl_k^2}l^2, \tag{7}$$

$$x(l)=l-\frac{2}{63R^2l_k^4}l^7+\frac{2}{3159R^4l_k^8}l^{13}-\frac{4}{623295R^6l_k^{12}}l^{19}, \tag{8}$$

$$y(l)=\frac{1}{6Rl_k^2}l^4-\frac{2}{405R^3l_k^6}l^{10}+\frac{1}{1458R^5l_k^{10}}l^{16}; \tag{9}$$

  - within $l\in\left\langle\frac{l_k}{2},l_k\right\rangle$:

$$k(l)=-\frac{1}{R}+\frac{4}{Rl_k}l-\frac{2}{Rl_k^2}l^2 \tag{10}$$

$$\begin{aligned}x(l)=&\,x\left(\frac{l_k}{2}\right)+\cos\left(\frac{l_k}{12R}\right)\left(l-\frac{l_k}{2}\right)-\frac{1}{4R}\sin\left(\frac{l_k}{12R}\right)\left(l-\frac{l_k}{2}\right)^2\\&-\left[\frac{1}{24R^2}\cos\left(\frac{l_k}{12R}\right)+\frac{1}{3Rl_k}\sin\left(\frac{l_k}{12R}\right)\right]\left(l-\frac{l_k}{2}\right)^3\\&+\left[\left(\frac{1}{192R^3}+\frac{1}{6Rl_k^2}\right)\sin\left(\frac{l_k}{12R}\right)-\frac{1}{8R^2l_k}\cos\left(\frac{l_k}{12R}\right)\right]\left(l-\frac{l_k}{2}\right)^4\\&-\left[\frac{1}{40R^3l_k}\sin\left(\frac{l_k}{12R}\right)+\left(\frac{1}{1920R^4}-\frac{1}{30R^2l_k^2}\right)\cos\left(\frac{l_k}{12R}\right)\right]\left(l-\frac{l_k}{2}\right)^5,\end{aligned} \tag{11}$$

$$y(l)=y\left(\frac{l_k}{2}\right)-\sin\left(\frac{l_k}{12R}\right)\left(l-\frac{l_k}{2}\right)+\frac{1}{4R}\cos\left(\frac{l_k}{12R}\right)\left(l-\frac{l_k}{2}\right)^2$$
$$-\left[\frac{1}{24R^2}\sin\left(\frac{l_k}{12R}\right)-\frac{1}{3Rl_k}\cos\left(\frac{l_k}{12R}\right)\right]\left(l-\frac{l_k}{2}\right)^3$$
$$-\left[\left(\frac{1}{192R^3}-\frac{1}{6Rl_k^2}\right)\cos\left(\frac{l_k}{12R}\right)+\frac{1}{8R^2l_k}\sin\left(\frac{l_k}{12R}\right)\right]\left(l-\frac{l_k}{2}\right)^4$$
$$+\left[\left(\frac{1}{1920R^4}-\frac{1}{30R^2l_k^2}\right)\sin\left(\frac{l_k}{12R}\right)-\frac{1}{40R^3l_k}\cos\left(\frac{l_k}{12R}\right)\right]\left(l-\frac{l_k}{2}\right)^5; \quad (12)$$

- for the Bloss curve:

$$k(l)=\frac{3}{Rl_k^2}l^2-\frac{2}{Rl_k^3}l^3, \quad (13)$$

$$x(l)=l-\frac{1}{14R^2l_k^4}l^7+\frac{1}{16R^2l_k^5}l^8-\frac{1}{72R^2l_k^6}l^9, \quad (14)$$

$$y(l)=\frac{1}{4Rl_k^2}l^4-\frac{1}{10Rl_k^3}l^5-\frac{1}{60R^3l_k^6}l^{10}+\frac{1}{44R^3l_k^7}l^{11}; \quad (15)$$

- for the cosine curve:

$$k(l)=\frac{1}{2R}-\frac{1}{2R}\cos\left(\frac{\pi}{l_k}l\right), \quad (16)$$

$$x(l)=l-\frac{\pi^4}{2016R^2l_k^4}l^7+\frac{\pi^6}{25920R^2l_k^6}l^9-\frac{41\pi^8}{26611200R^2l_k^8}l^{11}, \quad (17)$$

$$y(l)=\frac{\pi^2}{40Rl_k^2}l^4-\frac{\pi^4}{1440Rl_k^4}l^6+\frac{\pi^6}{80640Rl_k^6}l^8-$$
$$+\frac{1}{10}\left(\frac{\pi^6}{10368R^3l_k^6}+\frac{\pi^8}{725760Rl_k^8}\right)l^{10}; \quad (18)$$

- for the sine curve:

$$k(l)=\frac{1}{Rl_k}l-\frac{1}{2\pi R}\sin\left(\frac{2\pi}{l_k}l\right), \quad (19)$$

$$x(l)=l-\frac{\pi^4}{648R^2l_k^6}l^9+\frac{\pi^6}{2970R^2l_k^8}l^{11}-\frac{29\pi^8}{737100R^2l_k^{10}}l^{13}, \quad (20)$$

$$y(l)=\frac{\pi^2}{30Rl_k^3}l^5-\frac{\pi^4}{315Rl_k^5}l^7+\frac{\pi^6}{5670Rl_k^7}l^9-\frac{\pi^8}{155925Rl_k^9}l^{11}. \quad (21)$$

Theoretical analyses and experimental studies, e.g. [15–17, 22], unequivocally indicate lower (and therefore more favourable) dynamic interactions during train runs on smooth transition curves. However, in spite of its undisputed advantages, the scope of application of these curves in the operated railway tracks is, to a large extent, limited. There is an opinion that their correct delineation in the field is very difficult due to very small values of horizontal ordinates (and ordinates of gradient due to cant) in the initial region. They result from excessive resmoothing of the curvature diagram in this region. In practice, this leads to shortening of the transition curve (i.e. elongation of the adjacent straight) in relation to the design assumptions. It seems that this issue should be looked at more closely.

Two geometric systems of transition curves for the speed V = 160 km/h, the characteristics of which are presented in Table 1, were considered in the comparative analysis. The following limit values of kinematic parameters were adopted: unbalanced acceleration on a circular curve a_{per} = 0.85 m/s^2, acceleration increment ψ_{per} = 0.3 m/s^3 and wheel lifting speed on the gradient due to cant f_{per} = 28 mm/s. The first system (R = 1850 m, h_0 = 60 mm) Two geometric systems

Table 1

List of characteristic values for the transient curves under consideration

System	R [m]	h_0 [mm]	a_m [m/s^2]	Type of transition curve	l_k [m]	ψ_{max} [m/s^3]	f_{max} [mm/s]
I	1850	60	0.675	Clothoid	100	0.300	26.67
				Fourth-degree parabola	200	0.300	26.67
				Bloss curve	150	0.300	26.67
				Cosine curve	158	0.298	26.51
				Sine curve	200	0.300	26.67
II	1250	115	0.828	Clothoid	183	0.201	27.93
				Fourth-degree parabola	365	0.201	28.01
				Bloss curve	274	0.201	27.98
				Cosine curve	287	0.201	27.97
				Sine curve	365	0.201	28.01

[Own study].

Table 2

Values of horizontal ordinates *y*[mm] of the transition curves from Table 1 of System I over the first 20-m section

L [m]	Clothoid	Fourth-degree parabola	Bloss curve	Cosine curve	Sine curve
0	0	0	0	0	0
2	0.0072	0.00004	0.00010	0.00007	0.000001
4	0.0577	0.00058	0.00152	0.00114	0.00002
6	0.1946	0.00292	0.00766	0.00577	0.00017
8	0.4613	0.00293	0.02408	0.01822	0.00073
10	0.9009	0.02252	0.05846	0.04446	0.00222
12	1.5568	0.04670	0.12056	0.09214	0.00551
14	2.4721	0.08652	0.22211	0.17059	0.01190
16	3.6901	0.14760	0.37682	0.29080	0.02317
18	5.2541	0.23643	0.60022	0.46538	0.04168
20	7.2072	0.36036	0.90971	0.70860	0.07047

[Own study].

of transition curves for the speed V = 160 km/h, the characteristics of which are presented in Table 1, were considered in the comparative analysis. The following limit values of kinematic parameters were adopted: unbalanced acceleration on a circular curve a_{per} = 0.85 m/s^2, acceleration increment ψ_{per} = 0.3 m/s^3 and wheel lifting speed on the gradient due to cant f_{per} = 28 mm/s. The first system (R = 1850 m, h_0 = 60 mm) tried to achieve the shortest possible length of the transition curve by using a relatively small cant on a circular curve (the longer the curve length, the smaller the values of horizontal ordinates). In the second system (R = 1250 m, h_0 = 115 mm) the radius of the curve R, was reduced, which made it necessary to introduce a larger cant and consequently led to an increase in the length of transition curves.

Table 2 gives the values of the horizontal ordinates of the transition curves in Table 1 of System I for the first 20 m section. Figure 2 provides a suitable graphic illustration. Figure 3 shows the percentage values of the ratio of the horizontal ordinates of the smooth transition curves to the ordinates of the clothoid in the initial region.

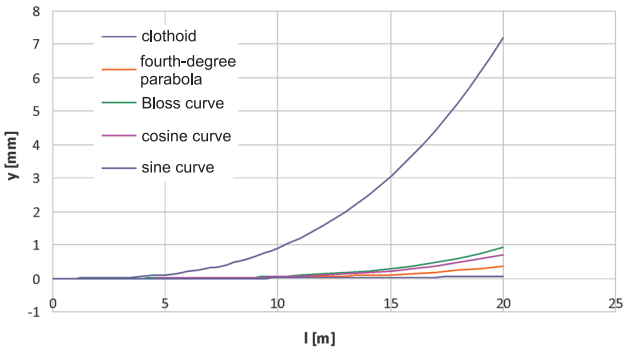

Fig. 2. Diagrams of horizontal ordinates of transition curves from System I in Table 1 in the first 20-m section [own study]

As can be seen, in this case the horizontal ordinates of smooth transition curves in the initial region are very small. For the first 10 m they are a fraction of a millimetre, at 20 m they do not yet reach 1 mm (0.1 mm for the sine curve). It is difficult to imagine the practical implementation of these transition curves, especially the sine curve, the ordinate of which for l = 20 m constitutes only 1% of the clothoid ordinate (Fig. 3).

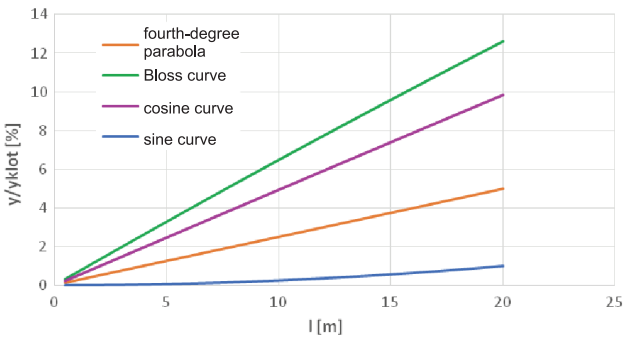

Fig. 3. Percentage values of the ratio of horizontal ordinates of smooth transition curves to clothoid ordinates in the initial region for System I in Table 1 [own study]

The presented remarks also apply to the gradient due to cant. In Table 3, the values of the gradient due to cant ordinates on transition curves from System I in Table 1 over the first 20 m section are given, and in Figure 4 the appropriate graphic illustration is presented.

Over the first 10 m, the gradient due to cant ordinates shall in no case exceed 1 mm. After 20 m they reach almost 3 mm for the Bloss curve and about 2.5 mm for the cosine curve. The smallest values of the gradient due to cant ordinates occur on the sine curve – after 20 m it is about 0.4 mm.

Table 3

The gradient due to cant ordinate values *h* [mm] on transition curves from System I in Table 1 over the first 20-m section

L [m]	Clothoid	Fourth-degree parabola	Bloss curve	Cosine curve	Sine curve
0	0	0	0	0	0
2	1,2000	0,0120	0,0317	0,0237	0,0004
4	2,4000	0,0480	0,1257	0,0948	0,0032
6	3,6000	0,1080	0,2803	0,2132	0,0106
8	4,8000	0,1920	0,4938	0,3787	0,0252
10	6,0000	0,3000	0,7644	0,5911	0,0491
12	7,2000	0,4320	1,0906	0,8499	0,0847
14	8,4000	0,5880	1,4704	1,1549	0,1341
16	9,6000	0,7680	1,9024	1,5054	0,1996
18	10,8000	0,9720	2,3846	1,9010	0,2832
20	12,0000	1,2000	2,9156	2,3410	0,3871

[Own study].

Table 4

The values of the horizontal ordinates *y* [mm] of the transition curves in Table 1 of System II over the first 20-m section

L [m]	Clothoid	Fourth-degree parabola	Bloss curve	Cosine curve	Sine curve
0	0	0	0	0	0
2	0,00583	0,00002	0,00004	0,00003	0,0000002
4	0,04663	0,00026	0,00068	0,00051	0,0000055
6	0,15738	0,00130	0,00342	0,00251	0,000042
8	0,37304	0,00410	0,01078	0,00818	0,000177
10	0,72860	0,01001	0,02625	0,01996	0,00054
12	1,25902	0,02075	0,05427	0,04139	0,00134
14	1,99927	0,03845	0,10025	0,07666	0,00291
16	2,98433	0,06559	0,17051	0,13074	0,00566
18	4,24918	0,10506	0,27230	0,20937	0,01020
20	5,82878	0,16013	0,41379	0,31901	0,01727

[Own study].

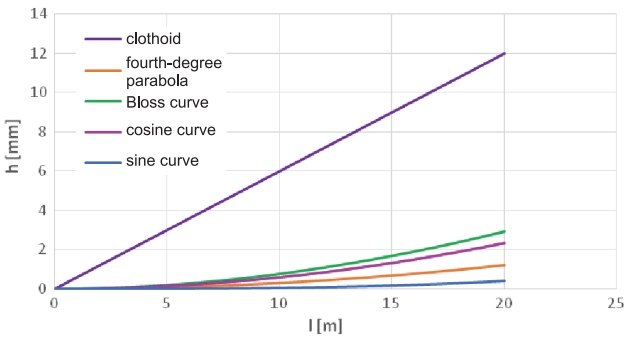

Fig. 4. Diagrams of the gradient due to cant ordinates on transition curves from System I in Table 1 over the first 20-m section [own study]

The calculated values of horizontal ordinates for the second case under consideration, i.e. for System II in Table 1, are presented in Table 4. The graphs of these ordinates are presented in Figure 5. Figure 6 shows the percentage values of the ratio of horizontal ordinates of smooth transition curves to the ordinates of the clothoid in the initial region.

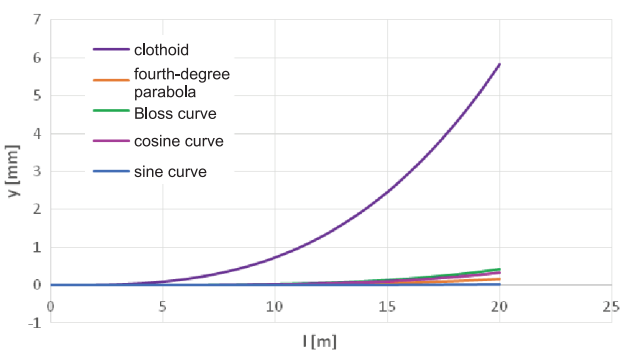

Fig. 5. Diagrams of horizontal ordinates of transition curves from System II in Table 1 in the first 20-m section [own study]

Table 5

The gradient due to cant ordinates *h* [mm] on transition curves from System II in Table 1 over the first 20-m section

L [m]	Clothoid	Fourth-degree parabola	Bloss curve	Cosine curve	Sine curve
0	0	0	0	0	0
2	1,2568	0,0069	0,0183	0,0138	0,00012
4	2,5137	0,0276	0,0728	0,0551	0,0010
6	3,7705	0,0622	0,1630	0,1240	0,0034
8	5,0273	0,1105	0,2884	0,2203	0,0080
10	6,2842	0,1726	0,4484	0,3441	0,0155
12	7,5410	0,2486	0,6424	0,4954	0,0268
14	8,7978	0,3384	0,8700	0,6739	0,0426
16	10,0546	0,4420	1,1306	0,8796	0,0635
18	11,3115	0,5594	1,4237	1,1125	0,0903
20	12,5683	0,6906	1,7487	1,3725	0,1238

[Own study].

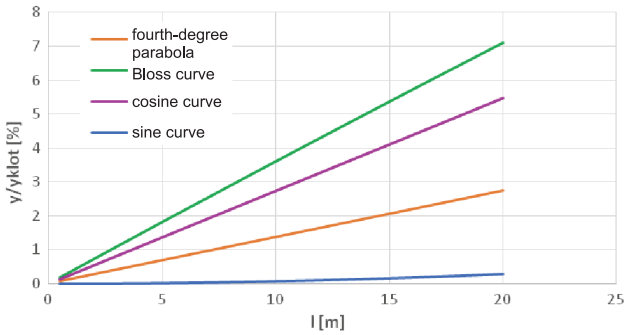

Fig. 6. Percentage values of the ratio of horizontal ordinates of smooth transition curves to clothoid ordinates in the initial region for System II in Table 1 [own study]

As can be seen, for System II in Table 1 (i.e. R = 1250 m, h_0 = 115 mm) the situation is even worse than for System I (R = 1850 m, h_0 = 60 mm). The ordinates of the horizontal smooth transition curves in the initial region are very small; after 20 m they do not reach even 0.5 mm (0.02 mm for sine curve). In Figure 6, the ratio of horizontal ordinates for the clothoid after 20 m reaches 7% for the Bloss curve, while for the sine curve it is only 0.3%. This is undoubtedly due to the use of longer transition curves, which was due to the higher cant value on the circular curve and the need to maintain the f_{per} value.

Table 5 shows the gradient due to cant ordinates on transition curves from System II in Table 1 for the first 20 m, and Figure 7 shows a suitable graphic illustration.

As shown in Table 4, the gradient due to cant ordinates on smooth transition curves are approximately twice as small as in System I, although the cant on a circular curve is h_0 = 115 mm (previously h_0 = 60 mm). Over the first 10 m, the gradient due to cant ordinates on these curves do not exceed 0.5 mm and after 20 m they are less than 2 mm. The smallest gradient due to cant ordinates occur, as before, on the sine curve and after 20 m they are slightly greater than 0.1 mm.

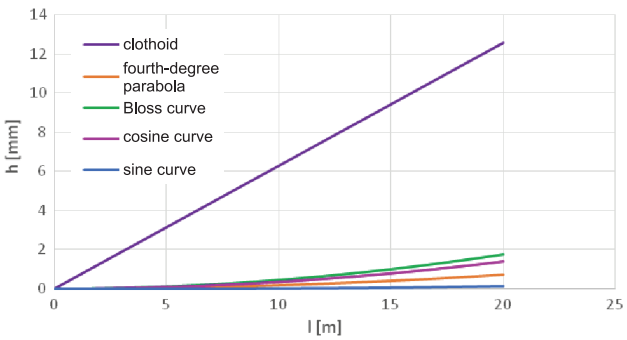

Fig. 7. Diagrams of the gradient due to cant ordinates on transition curves from System II in Table 1 over the first 20 m section [own study]

Although the analysis was conducted on a random basis, its conclusions seem to be clear. In most cases, it is very difficult, if not impossible, to properly shape the initial region of smooth transition curves. Horizontal ordinates of a fraction of a millimetre may pose a serious problem both in execution and later maintenance (especially in the case of ballast pavement).

Since the smooth transition curves in the initial region lead to very small values of horizontal ordinates, the possible modification should not differ too much from the shape of the clothoid in this region (the ordinates of which are not too big either). It should, however, cover the central region of the transition curve (by introducing non-linear curvature) and the region of the entrance to the circular curve. Of course, one should also strive to obtain the smallest possible length of the new solution in comparison with the length of the base curve (clothoid).

4. Proposal for a new transition curve for railway roads

The general method of identification of curvature $k(l)$ on transition curves [17] shows that for the radius R of circular curve and length l_k of transition curve the assumed assumptions determine the following limits:

$$\begin{cases} k(0)=0, \quad k\left(l_k\right)=\dfrac{1}{R}, \\ k'(0)=\dfrac{C}{Rl_k}, \quad k'\left(l_k\right)=0, \end{cases} \tag{22}$$

and the differential equation:

$$k^{(4)}(l)=0 \tag{23}$$

whereby the numerical factor $C \geq 0$. Conditions (22) for $C = 0$ apply to the Bloss curve. The solution to the differential problem (22), (23) gives the general equation of curvature:

$$k(l) = \frac{C}{Rl_k} l - \frac{2C-3}{Rl_k^2} l^2 + \frac{C-2}{Rl_k^3} l^3. \tag{24}$$

A detailed analysis elaborated in one paper [20] and in a paper for the INFRASZYN 2019 conference [21] showed that the most advantageous solution was the ratio value of $C = 1$, because in this case the length corresponding to the transition curve must be greater than the clothoid one by only 1/3. Assuming $C = 1$ leads to the following function equation $k(l)$:

$$k(l)=\frac{1}{Rl_k}l+\frac{1}{Rl_k^2}l^2-\frac{1}{Rl_k^3}l^3. \tag{25}$$

As can be seen, the first equation segment (25) takes a linear form, representing the curvature of the clothoid. The other two segments are non-linear – they occur in the second and third power, i.e. similarly to the Bloss curve. The angle of tangent slope $\Theta(l)$ is described by the equation

$$\Theta(l)=\frac{1}{2Rl_k}l^2+\frac{1}{3Rl_k^2}l^3-\frac{1}{4Rl_k^3}l^4. \tag{26}$$

whereby at the end of the transition curve its value is $\Theta\left(l_k\right)=\dfrac{7}{12R}l_k$. Knowing this angle allows tangents to be reconciled with the next geometric element. Coordinate equations of the sought transition curve can be written in the parametric form [17]:

$$x(l)=\int \cos\Theta(l)dl, \tag{27}$$

$$y(l)=\int \sin\Theta(l)dl. \tag{28}$$

To develop the functions $\cos\Theta(l)$ and $\sin\Theta(l)$ in the Maclaurin series, the Maxima package [23] was used, and then individual parts were integrated, obtaining parametric equations:

$$\begin{aligned} x(l) &= l-\frac{1}{40R^2l_k^2}l^5-\frac{1}{36R^2l_k^3}l^6+\frac{5}{504R^2l_k^4}l^7+ \\ &+\frac{1}{96R^2l_k^5}l^8+\left(\frac{1}{3456R^4l_k^4}-\frac{1}{288R^2l_k^6}\right)l^9, \end{aligned} \tag{29}$$

$$\begin{aligned} y(l) &= \frac{1}{6Rl_k}l^3+\frac{1}{12Rl_k^2}l^4-\frac{1}{20Rl_k^3}l^5- \\ &+\frac{1}{336R^3l_k^3}l^7-\frac{1}{192R^3l_k^4}l^8+\frac{1}{2592R^3l_k^5}l^9. \end{aligned} \tag{30}$$

At the beginning, equations (29) and (30) are consistent with the parametric equations of the clothoid. The first two parts from equation (5) are the same as in equation (29), while the first part of equation (30) is identical to the first part of equation (6).

For the determined transition curve, the function equations $g(l)$ and $\dfrac{d}{dl}g(l)$ are as follows:

$$g(l)=\frac{l}{l_k}+\left(\frac{l}{l_k}\right)^2-\left(\frac{l}{l_k}\right)^3, \frac{d}{dl}g(l)=\frac{1}{l_k}\left[1+2\frac{l}{l_k}-3\left(\frac{l}{l_k}\right)^2\right],$$

hence:

$$\psi(l)\cdot\frac{3,6l_k}{a_mV}=f(l)\cdot\frac{3,6l_k}{h_0V}=1+2\frac{l}{l_k}-3\left(\frac{l}{l_k}\right)^2$$

The formation of $\psi(l)\cdot\dfrac{3,6l_k}{a_mV}=f(l)\cdot\dfrac{3,6l_k}{h_0V}$ on the length of the new transition curve, against the background of the clothoid and the Bloss curve, is shown in Figure 8.

Exceeding ψ and f on the clothoid takes place for $l/l_k \in \left(0;0,667\right)$. The elongation of the described curve in relation to the clothoid, resulting from the highest value of exceeding ψ and f, is determined by the coefficient $A = 4/3$. Figure 9 shows curvature diagrams in the length of the clothoid and the Bloss curve in the geometric system marked as System I (Table 1) and in the length of the new transition curve of the corresponding length $l_k = 134$ m. Figure 10 presents graphs of horizontal ordinates for the curves mentioned above.

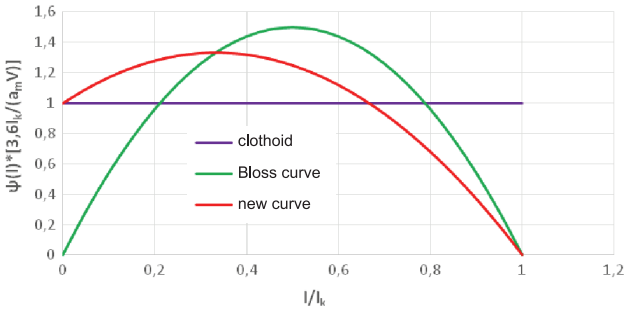

Fig. 8. The formation of $\psi(l)\cdot\frac{3,6l_k}{a_mV}\left(f(l)\cdot\frac{3,6l_k}{h_0V}\right)$ on the length of the clothoid, the Bloss curve and the new transition curve [own study]

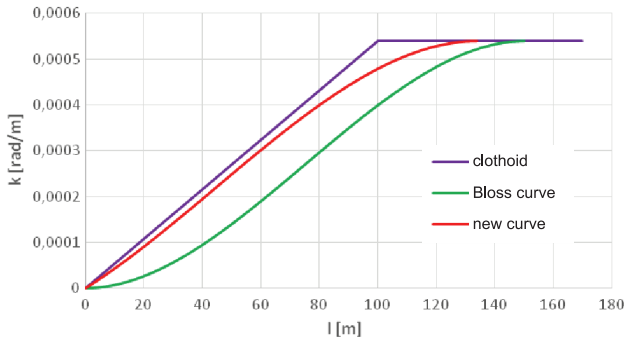

Fig. 9. Curvature graphs on the length of the clothoid, the Bloss curve and the new transition curve in System I from Table 1 [own study]

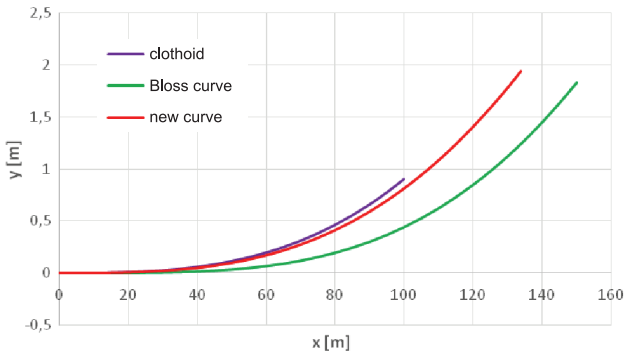

Fig. 10. Diagrams of horizontal ordinates on the length of the clothoid, the Bloss curve and new transition curve in System I from Table 1 (in the non-uniform scale) [own study]

As Figure 9 shows, the curvature diagram for the new transition curve significantly deviates from the curvature diagram for the Bloss curve. This is especially true for the initial zone, where the difference is formed and makes the curves so divergent from each other. On the other hand, the course of the curvature diagram for the new curve is significantly similar in length (although slightly more favourable) to the curvature diagram for the clothoid. Only in the final region, at the transition from a transition curve to a circular curve, is a significant difference visible: the curvature diagram for the new curve is much milder there.

It should be noted that the determined transition curve does not provide a smooth transition from a straight line to a transition curve, since at its starting point there is a deflection in the curvature diagram (Figure 9). It cannot therefore be classified as a standard smooth transition curve. As it is shorter than these curves and was designed to meet regulatory requirements, there is no doubt that it is of greater practical suitability for use. This can be confirmed by a detailed analysis of the horizontal ordinates of transition curve and gradient due to cant ordinates in the initial region.

5. Analysis of horizontal and gradient due to cant ordinates in the initial region of the new transition curve

To evaluate the values of the horizontal ordinates and the gradient due to cant ordinates in the initial region of the new transition curve, the first 20-m section was considered as in Chapter 3. In the analysis, two curves from Table 1 were taken into account – the clothoid and the Bloss curve, and the new transition curve against their background. The corresponding numerical values are shown in Table 6.

Figure 11 shows the horizontal ordinates of the above transition curves over the first 20 m section of System I (i.e. for the velocity $V = 160$ km/h and the radius $R = 1850$ m). Figure 12 shows the percentage values of the ratio of horizontal ordinates of these curves to the ordinates of the clothoid in the initial region.

As can be seen, the horizontal ordinates of the Bloss curve representing smooth transition curves in the initial region are small, as already shown in Figure 2. They do not even reach 1 mm after 20 m. The percentage ratio of the ordinates of this curve to the clothoid varies from 1% to less than 13%, while for the new transition curve it ranges from 75 to 80%. Therefore, the implementation possibilities in this zone of the new transition curve do not differ much from the analogous possibilities in relation to the clothoid.

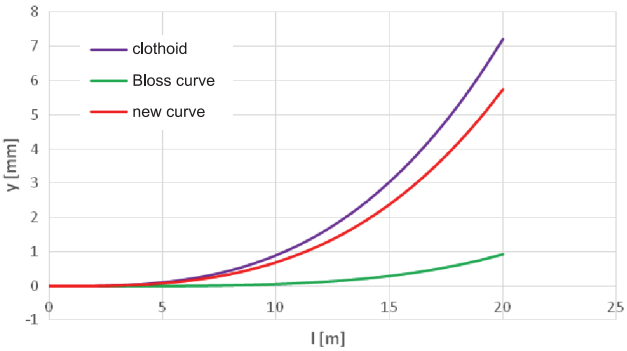

Fig. 11. Horizontal ordinates of the clothoid, the Bloss curve and the new transition curve on the first 20-m section in System I [own study]

Table 6

Selected values of horizontal ordinates *y* [mm] and the gradient due to cant ordinates *h* [mm] in the initial region of selected transition curves

System I		V = 160 km/h		R = 1850 m		h_0 = 60 mm	
		l = 1 m	l = 3 m	l = 5 m	l = 10 m	l = 15 m	l = 20 m
	y	0.000901	0.024324	0.112613	0.900901	3.040541	7.207208
Clothoid l_k = 100 m	h	0.600000	1.800000	3.000000	6.000000	9.000000	12.00000
The Bloss curve l_k = 150 m	y	0.000006	0.000483	0.003704	0.058458	0.291892	0.909710
	h	0.007964	0.071040	0.195556	0.764444	1.680000	2.915556
The new transition curve l_k = 134 m	y	0.000675	0.018353	0.085572	0.696277	2.387530	5.743949
	h	0.451078	1.372684	2.319226	4.786826	7.384095	10.09233
System II		V = 160 km/h		R = 1250 m		h_0 = 115 mm	
		l = 1 m	l = 3 m	l = 5 m	l = 10 m	l = 15 m	l = 20 m
Clothoid l_k = 183 m	y	0.000729	0.001967	0.091075	0.728597	2.459016	5.828780
	h	0.628415	1.885246	3.142077	6.284153	9.426230	12.56831
The Bloss curve l_k = 274 m	y	0.000003	0.000215	0.001653	0.026251	0.131910	0.413790
	h	0.004584	0.041056	0.113486	0.448353	0.996217	1.748690
The new transition curve l_k = 244 m	y	0.000548	0.014844	0.068977	0.557370	1.898860	4.541937
	h	0.473235	1.431105	2.438580	4.898359	7.477565	10.13554

[Own study].

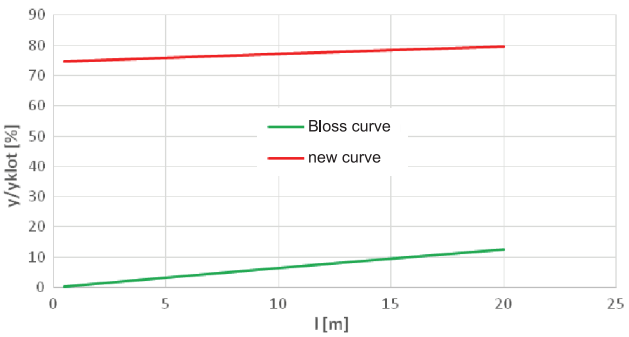

Fig. 12. Percentage values of the ratio of horizontal ordinates of the Bloss curve and the new transition curve to the clothoid ordinates in the initial region of System I [own study]

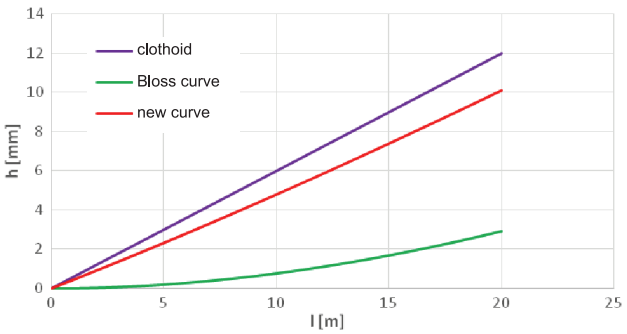

Fig. 13. Diagrams of the gradient due to cant ordinates for the clothoid, the Bloss curve and the new transition curve for the first 20 m of System I [own study]

The presented remarks also apply to the gradient due to cant (Fig. 13). The gradient due to cant ordinates for the Bloss curve are much smaller than the corresponding values for the clothoid and the new transition curve and are impossible to practically implement for the first 10 m.

Diagrams of horizontal ordinates for System II, i.e. for velocity V = 160 km/h and radius R = 1250 m, are shown in Figure 14. Figure 15 shows the percentage ratio of horizontal ordinates of these curves to the ordinates of the clothoid in the initial region, while graphs of the gradient due to cant ordinates are shown in Figure 16.

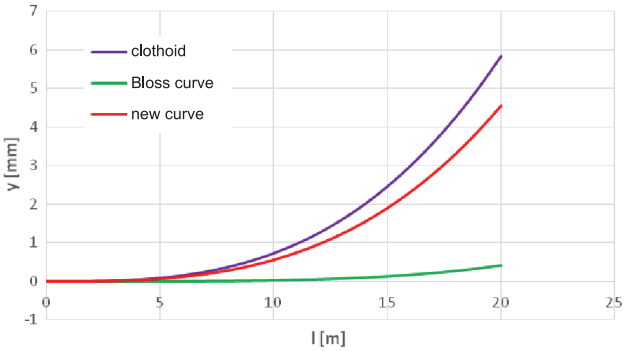

Fig. 14. Diagrams of horizontal ordinates of the clothoid, the Bloss curve and the new transition curve on the first 20 m in System II [own study]

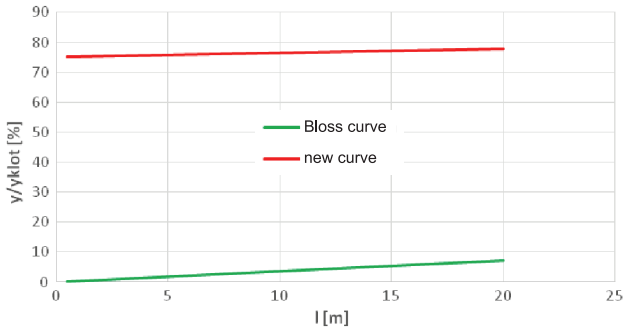

Fig. 15. Percentage values of the ratio of horizontal ordinates of the Bloss curve and the new transition curve to the clothoid ordinates in the initial region of System II [own study]

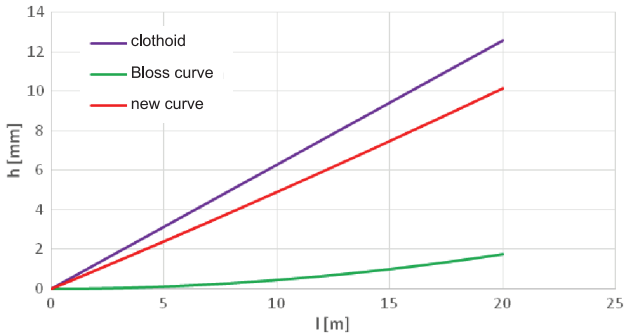

Fig. 16. Diagrams of the gradient due to cant ordinates for the clothoid, the Bloss curve and the new transition curve for the first 20 m of System II [own study].

As can be seen, for velocity $V = 160$ km/h and radius $R = 1850$ m, the horizontal ordinates in the initial region are even smaller than in the previous case. The horizontal ordinates of the Bloss curve per 20 m do not even reach 0.5 mm and the ordinates of the gradient due to cant are also very small. The corresponding values for the new transition curve are slightly smaller than for the clothoid.

Thus, for the Bloss curve, the practical implementation and subsequent maintenance of very small horizontal ordinates and the gradient due to cant ordinates in the initial area does not seem possible. However, the implementation possibilities of the initial zone of the new transition curve are analogous to those of the clothoid.

The presented new transition curve could successfully compete with the commonly used transition curve in the form of a clothoid. It is similar to it in the initial region, but it differs significantly in its further length, especially in the final region, where it provides a gentle entry from a transition curve into a circular curve. This creates a significant advantage of the new geometric solution presented in the article from the point of view of dynamic properties in the track – rail vehicle system.

6. Conclusions

On railway roads, the mutual comparison of transition curves requires certain assumptions regarding the binding values of permissible kinematic parameters – the acceleration increment ψ and the speed of raising the rolling stock wheel on the gradient due to cant f. There is an intuitive conviction that curves with non-linear curvature change on the length (i.e. smooth transition curves) may be subject to much higher (even doubled) permissible values than for the clothoid (with linear curvature). This was even reflected in the binding regulations. In this article, it has been unequivocally demonstrated that, on smooth transition curves, exceeding the values of ψ and f occurring on the clothoid is not local (point), but covers at least half of their length, and the value of this excess is significant. Therefore, it seems appropriate to maintain, for all types of transitional curves, the same rules concerning the limit values for kinematic parameters.

Smooth transition curves have been known for a long time and have many undisputed advantages – first of all, they are characterized by lower values of dynamic interactions than is the case with a clothoid. However, the scope of their use on railway roads has been very limited so far. Unfortunately, these curves have one fundamental disadvantage – very small values of horizontal ordinates (and gradient due to cant ordinates) in the initial region, in practice often impossible to implement and maintain. This was confirmed in the analysis of the problem carried out within the framework of this study.

It was therefore considered that the root cause of the problems encountered with regard to smooth transition curves is the excessive softening of the curvature in their initial region. Using the method of curvature identification by means of differential equations, a new form of transition curve was obtained, abandoning the condition of zeroing the curvature derivative at the initial point.

The new transition curve is characterized by a mild curvature in the area of the entrance to the circular curve and its certain disturbance in the initial region (smaller, however, than in the case of a clothoid). It was shown that the new curve (from the implementation point of view) has a decisive advantage over the Bloss curve representing smooth transition curves. The implementation possibilities of this curve in the initial zone do not differ too much from the analogous possibilities in relation to a clothoid.

It seems that the presented new transition curve could successfully compete with the currently commonly used transition curve in the form of a clothoid. It is similar to it in the initial region, but it is significantly different in its further length, especially in the

final region, where it provides a gentle entry from a transition curve into a circular curve. This creates a significant advantage of the new geometric solution presented in the article from the point of view of dynamic properties in the track – rail vehicle system.

The issues described in this article appear to be relevant as other possibilities for improving the existing situation are largely limited. The demonstrated lack of practical implementation and maintenance of the ordinates of the transition curve and the ordinates of the gradient due to cant in the initial region significantly undermines the purposefulness of using the standard smooth transition curves on railway lines.

Literature

1. Arslan A. et.al.: *Transition curve modeling with kinematical properties: research on log-aesthetic curves*, Computer-Aided Design and Applications, *v*ol. 11, no. 5/2014, Taylor & Francis Online, pp. 509–517.
2. Bałuch H.: *Optymalizacja układów geometrycznych toru* [Optimisation of track geometry], Wydawnictwa Komunikacji i Łączności, Warszawa, 1983.
3. Baykal O. et.al.: *New transition curve joining two straight lines*, Journal of Transportation Engineering, ASCE, 1997, vol. 123, no. 5, pp. 337–345.
4. Bosurgi G., D'Andrea A.: *A polynomial parametric curve (PPC-CURVE) for the design of horizontal geometry of highways*, Computer-Aided Civil and Infrastructure Engineering, Wiley Online, 2012, vol. 27, no. 4/, pp. 303–312.
5. Cai H., Wang G.: *A new method in highway route design: joining circular arcs by a single C-Bezier curve with shape parameter*, Journal of Zhejiang University SCIENCE A, Springer, 2009, vol. 10, no. 4, pp. 562–569.
6. Grabowski R.J.: *Gładkie przejścia krzywoliniowe w drogach kołowych i kolejowych* [Smooth radii of curves on roads and railways], Zeszyty Naukowe Akademii Górniczo-Hutniczej, Kraków, 1984, z. 82.
7. Habib Z., Sakai M.: *G^2 Pythagorean hodograph quintic transition between two circles with shape control*, Computer Aided Geometric Design, Elsevier, 2007, vol. 24, pp. 252–266.
8. Habib Z., Sakai M.: *On PH quantic spirals joining two circles with one circle inside the other*, Computer-Aided Design, Elsevier, 2007, vol. 39, pp.125–132.
9. Hasslinger H.: *Measurement proof for the superiority of a new track alignment design element, the so-called "Viennese Curve"*, ZEVrail, Berlin, 2005.
10. Kobryń A.: *Polynomial solutions of transition curves*, Journal of Surveying Engineering ASCE, 2011, vol. 137, no. 3, 71–80.
11. Kobryń A.: *New solutions for general transition curves*, Journal of Surveying Engineering ASCE, 2014, vol. 140, no. 1, pp.12–21.
12. Kobryń A.: *Universal solutions of transition curves*, Journal of Surveying Engineering ASCE, 2016, vol. 142, no. 4, Article ID 04016010.
13. Kobryń A.: *Transition Curves for Highway Geometric Design*, Springer International Publishing, Series: Springer Tracts on Transportation and Traffic, 2017, vol. 14.
14. Kobryń A.: *Transition curves in vertical alignment as a method for reducing fuel consumption*, The Baltic Journal of Road and Bridge Engineering, Vilnius Gediminas Technical University (Lithuania), 2014, vol. 9, no. 4, pp. 260–268.
15. Koc W.: *Krzywe przejściowe z nieliniowymi rampami przechyłkowymi w warunkach eksploatacyjnych PKP* [Transition curves with non-linear cant under PKP operational conditions] Zeszyty Naukowe Politechniki Gdańskiej, 1990, nr 462, s. 3–12.
16. Koc W.: *Elementy teorii projektowania układów torowych* [Elements of track system design theory], Wydawnictwo Politechniki Gdańskiej, Gdańsk, 2004.
17. Koc W.: *Analytical method of modelling the geometric system of communication route*, Mathematical Problems in Engineering, vol. 2014, Hindawi, Article ID 679817.
18. Koc W.: *Identification of transition curves in vehicular roads and railways*, Logistics and Transport, Międzynarodowa Szkoła Logistyki i Transportu we Wrocławiu, 2015, vol. 28, no. 4, pp. 31–42.
19. Koc W.: *Transition curve with smoothed curvature at its ends for railway roads*, Current Journal of Applied Science and Technology, SCIENDOMAIN International, Article no. CJAST.35006, 2017, vol. 22, iss. 3, pp. 1–10.
20. Koc W.: *New transition curve adapted to railway operational requirements*, Journal of Surveying Engineering, ASCE, vol. 145, iss. 3 – August 2019, pp. 04019009:1-11.
21. Koc W.: *Wygładzona krzywa przejściowa dla dróg kolejowych* [Smooth transition curve for railways], Przegląd Komunikacyjny, Stowarzyszenie Inżynierów i Techników Komunikacji RP, Warszawa, 2019, vol. 74, nr. 7, s. 12–17.
22. Koc W., Mieloszyk E.: *Analiza porównawcza wybranych krzywych przejściowych z wykorzystaniem modelu dynamicznego* [Comparative analysis of selected transition curves using a dynamic model], Archiwum Inżynierii Lądowej, Komitet Inżynierii Lądowej i Wodnej Polskiej Akademii Nauk, 1987, tom 33, z. 2, s. 239–261.
23. Maxima Package, WWW http://maksima.sourceforge.net [access 20.09.2019].
24. Mieloszyk E., Koc W.: *General dynamic method for determining transition curve equations*, Rail International – Schienen der Welt, UIC, 1991, vol. 22, no. 10, pp. 32–40.
25. Sanchez-Reyes J., Chacon J. M.: *Nonparametric Bezier reprezentation of polynomial transition*

curves, Journal of Surveying Engineering, vol. 144, no. 2/2018, ASCE, 10.1061/(ASCE)SU.1943-5428.0000251, 04018001.
26. Standardy Techniczne – szczegółowe warunki techniczne dla modernizacji lub budowy linii kolejowych do prędkości Vmax ≤ 200 km/h (dla taboru konwencjonalnego) / 250 km/h (dla taboru z wychylnym pudłem), tom I – Droga Szynowa (Załącznik ST-T1-A6: Układy geometryczne torów) [Technical Standards – Detailed technical specification for upgrading or building railway lines to Vmax ≤ 200 km/h (for conventional rolling stock) / 250 km/h (for titling rolling stock), vol. I – Track Road (Annex ST-T1-A6: Geometrical track systems], PKP Polskie Linie Kolejowe S.A., Warszawa, 2017.
27. Tari E., Baykal O.: *An alternative curve in the use of high speed transportation systems*, ARI – An International Journal for Physical and Engineering Sciences, Springer, 1998, vol. 51, no. 2, pp. 126–135.
28. Tari E., Baykal O.: *A new transition curve with enhanced properties*, Canadian Journal of Civil Engineering, Canadian Science Publishing, 2005, vol. 32, no. 5, pp. 913–923.
29. Tasci L., Kuloglu N.: *Investigation of a new transition curve*, The Baltic Journal of Road and Bridge Engineering, Vilnius Gediminas Technical University (Lithuania), 2011, vol. 6, no. 1, pp. 23–29.
30. Wojtczak R.: *Charakterystyka krzywej przejściowej Wiener Bogen* [Characteristics of the Wiener Bogen transition curve], Wydawnictwo Politechniki Poznańskiej, Archiwum Instytutu Inżynierii Lądowej, 2017, nr 25, s. 419–431.
31. Zboiński K., Woźnica P.: *Optimisation of the railway transition curves' shape with use of vehicle-track dynamical model*, Archives of Transport, Komitet Transportu Polskiej Akademii Nauk, 2010, vol. 22, no. 3, pp. 387–407.
32. Zboiński K., Woźnica P.: *Formation of polynomial railway transition curves of even degrees*, Prace Naukowe Politechniki Warszawskiej – Transport, 2014, z. 101, s. 189–202.
33. Ziatdinov R.: *Family of superspirals with completely monotonic curvature given in terms of Gauss hypergeometric function*, Computer Aided Geometric Design, Elsevier, 2012, vol. 29, no 7, pp. 510–518.